Available online at www.sciencedirect.com
SCIENCE DIRECT®
Physica C 415 (2004) 189–196
PHYSICA C
www.elsevier.com/locate/physc

Use of Bi-2223 multifilamentary tapes as RF coils for 1.5 T MRI application

Jing Yuan, G.X. Shen *, Chunsheng Wang, Bing Wu, Peng Qu

Department of Electrical and Electronic Engineering, The University of Hong Kong, Room 705, CYC Building, Pokfulam Road, Hong Kong

Received 26 May 2004; received in revised form 9 August 2004; accepted 27 August 2004

Abstract

High temperature superconducting tapes are potential materials for radio frequency coils in magnetic resonance imaging. They show advantages of much lower cost and easier fabrication over HTS thin film coils. Resistance of HTS tape coils in the magnetic field was evaluated and their quality factors were analyzed. A 50 mm in diameter HTS tape coil for 1.5 T high field MRI was demonstrated for phantom imaging. It obtained a 1.11-fold and a 1.36-fold SNR improvement over the same size copper coil at 77 K and 300 K respectively. Technical issues with HTS tape coils in practice were also discussed.

Keywords: HTS tapes; Magnetic resonance imaging; RF coil; Signal-to-noise ratio; Surface resistance; Critical current density

1. Introduction

Many high temperature superconducting (HTS) radio frequency (RF) coils for magnetic resonance imaging (MRI) have been reported in these years [1–7]. Although significant signal-to-noise ratios (SNRs) have been obtained with these HTS coils compared with normal metal coils, most of these coils are made of HTS thin films, such as YBCO films. In the aspect of the price-to-performance ratio, the high cost and complicated fabrication of present HTS thin films decrease their attractions and limit their large scale applications.

In order to decrease the cost of the present HTS film RF coils, commercialized bismuth based HTS tapes, such as Bi-2223 and Bi-2212 tapes, are attracting researchers' interests gradually as the potential choice for RF coils in MRI. Grasso et al. [8] measured the quality factors (Qs) of surface coils made by Bi-2223 tapes and observed that their Qs were not much less than the YBCO films. Jing et al. [9] investigated the Qs theoretically and

* Corresponding author. Tel.: +852 28578486; fax: +852 25598738.
E-mail address: gxshen@eee.hku.hk (G.X. Shen).

0921-4534/$ - see front matter © 2004 Elsevier B.V. All rights reserved.
doi:10.1016/j.physc.2004.08.014

verified it with experiments. Both of these investigations reported that HTS tape coils have potentials to obtain higher SNR than copper coils for imaging. Cheng et al. [10] built a 5-in. tape RF receiving coil for 0.21 T MRI system, and demonstrated a 3 times SNR improvement over an equivalent room temperature copper coil, which proved the feasibility of HTS tapes for MRI.

HTS tape coils show many advantages over present HTS film coils. First of all, the costs of tape coils can be much less than those of thin film coils due to the cheap material and easy fabrication. Secondly, HTS tapes can be fabricated, theoretically, to as large as possible, to improve RF penetration and increase imaging field of view (FOV). Thirdly, resonant frequencies of tape coils are easier to tune than film coils after fabrication. Furthermore, without the rigid substrate of films, HTS tapes have possibility to be implemented to not only surface coils, but also volume coils by winding, etching and molding [4,7]. On the other hand, tape coils also have their own drawbacks. They have higher resistance and lower Qs than film coils due to their not pure superconducting structures. The silver sheath of HTS tapes has to been removed [8] for imaging to avoid the complete screening of the superconducting phase from RF signal, which makes the bare tape quite brittle and hard to handle. In addition, HTS tapes cannot be used to build microcoils because their superconducting performance will degrade significantly when over-bended.

However, many questions about HTS tape coils still have not been fully discussed and many technical issues have not been well addressed. Since HTS tapes are often focused towards applications in the AC frequency range far below RF, their performance, especially their surface resistance at RF, is really an issue that has not been fully investigated. Due to the structure of superconducting grains and weak link Josephson junctions between them as well as of normal metal inclusions, surface resistance of HTS tapes, will increase in the magnetic field. Although HTS tape coil has been demonstrated for low field imaging, the experiments with HTS tape coils for high field imaging have not been carried out so far. In this work, these questions are analyzed theoretically, and a 50 mm Bi-2223 tape coil for phantom imaging at 1.5 T and its SNR performance are reported.

2. Theoretical analysis

2.1. Surface resistance

Surface resistance is one of the most important parameters for RF and microwave applications. It reflects the intrinsic loss of the material itself at high frequency. The surface resistance of the normal metal is a square root function of frequency resented as Eq. (1)

$$R_{\mathrm{srf}} = \sqrt{\frac{\mu_0 \omega \rho}{2}}, \tag{1}$$

where μ_0 denotes the permeability of free space, ω, the angular frequency and ρ the resistivity.

For superconductors, two-fluid model, as expressed in Eq. (2) [11], is widely used as a first-order approximation of the surface resistance of superconductors.

$$R_{\mathrm{srf}} = \frac{1}{2\rho_{\mathrm{n}}} \mu_0^2 \omega^2 \lambda^3 \left(\frac{T}{T_{\mathrm{c}}}\right)^4, \quad \text{where } \lambda = \lambda_0 \left(1 - \left(\frac{T}{T_{\mathrm{c}}}\right)^4\right)^{1/2}, \tag{2}$$

where ρ_{n} is the normal state resistivity, λ is the penetration depth, T is the operating temperature and T_{c} is the critical temperature of the superconductor. Penetration depth is much dependent on the crystal grain alignment but is believed to be frequency independent [12]. It was reported that the penetration depth in YBCO thick films with T_{c} of 92 K is approximately 3 μm at 77 K and only 0.15 μm [13] in high quality epitaxial thin films.

So far, most of the work on surface resistance of HTS films concentrates on microwave frequency range above 1 GHz. At the frequency range of interests for MRI, from 10 MHz to 400 MHz (corresponding to the magnetic field strength from about 0.25 T to 10 T), the calculation by two-fluid model often causes significant discrepancy, and it is difficult to measure the surface resistance of HTS films in cavities or using planar resonator due to the large size and the very high sensitivity

required to measure the low loss of films [12]. Therefore the evaluation of surface resistance has to been carried out by quality factor, Q, measurement of surface coil made of HTS films [12] and tapes [8,9]. According to reports in Refs. [1–3,6], the Q of a thin film can be as high as tens of thousand, but a HTS tape coil often has the Q of about a few thousand [8,10]. It indicates that the resistivity of a HTS thin film may be much lower than that of a HTS tape coil. However, when compared with Q of normal metal coils of about several hundred, HTS tape coils still show about one order higher Q, which indicates HTS tape has lower resistivity than normal metals. On the other hand, Bi-2223 tapes are not pure superconductor even after sheath removal. Therefore its surface resistance may perform like a parallel combination of superconducting filaments and silver inner matrix. Fortunately, it has been observed that close to the silver sheath, the conversion to the Bi-2223 is more complete and the grains are larger and more highly aligned than the central part in the tape [14]. Consequently, the current should almost concentrate in the HTS grains at the tape edges at RF range. But at higher frequency, it is expected that HTS tapes will demonstrate square root frequency dependence of surface resistance as shown in Eq. (1).

2.2. Resistance in the magnetic field

The resistance of HTS RF coils in the static magnetic field should be quite different from the resistance outside of the field. There are two approaches to investigate the resistance of HTS coils in the magnetic field.

One approach is to calculate the surface resistance based on some theoretical models. However, there is a big issue that the penetration depth is not only temperature dependent but also magnetic strength dependent. The dependence of penetration depth on the field strength is so complicated that there are still arguments on it. According to the work by Yip and Sauls [15] and by Maeda et al. respectively [16], the increase of penetration depth is proportional to the applied magnetic field, which is in sharp contrast to the square law expression by Sridhar et al. [17]. However, the applied field in Ref. [16] did not exceed 100 Oe (corresponding to 0.01 T), much lower than the magnetic field used in MRI. Therefore, the validity of the equation in the high field has not been verified.

The other approach is to use an effective resistivity to evaluate the HTS resistance in the magnetic field supposed that the resistivity is independent of the frequency. Therefore the resistance can be calculated by the well know equation as expressed in Eq. (3):

$$R = \frac{\rho_e l}{S}, \tag{3}$$

where ρ_e is the effective resistivity, l is the length and S is the transport cross section. The dependence of penetration depth on the frequency is related with the variation of transport cross section S.

Kusevic et al. [18] investigated the resistivity of the Bi-2223 tape with silver sheath in the magnetic field applied perpendicular to the tape surface from $0\,T$ to $15\,T$. It was found that throughout the explored field range, the resistivity shows Arrhenius behavior expressed as

$$\rho \propto \exp(-U^*(1 - T/T_{cs})/k_B T B^{0.5}) \quad 1T \leqslant B \leqslant 15T, \tag{4}$$

where T is the temperature, U^* is a constant determined by the specific tape sample, k_B is Boltzmann's constant, B is the magnetic field strength and $T_{cs} = 118$ K. According to the data in the field of 1.5 T, the resistivity of Bi-2223 HTS tape at 77 K should be in the order of $10^{-9}\,\Omega$m, the same order as the cool copper in liquid nitrogen. Accounting for the orientation of the tape with respect to the field direction, the field perpendicular to the tape surface in Kusevic's work [18] is an extreme situation in which case the resistivity should be the highest. In practice, the orientation of the HTS tape coil with respect to the magnetic field differs with position, which is demonstrated in Fig. 1. For example, at point A in Fig. 1, the magnetic field is perpendicular to the tape surface, whereas at point B, the field is parallel to the tape surface. In addition, the silver sheath removal may be helpful to reduce the resistivity of the tape coil in the imaging. Moreover, owing to the fast development of the Bi-2223 tapes, nowadays Bi-2223 tapes with

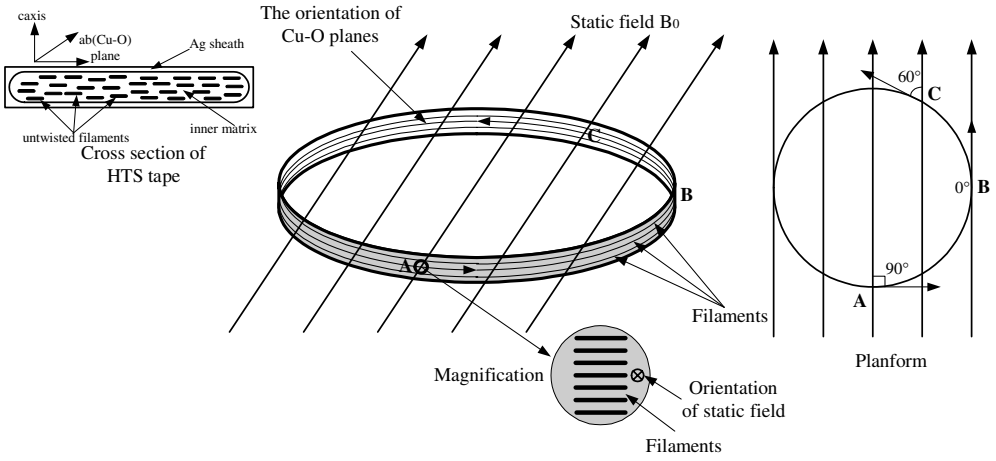

Fig. 1. The orientation of the Cu–O planes in the HTS tape filaments with respect to the static magnetic field differs with positions. For example, at points A and B, the Cu–O planes of HTS filaments are perpendicular and parallel to the static field B_0 respectively. At point C, the intersection angle between filaments and B_0 is 60°. The left section is the demonstration of the tape cross section.

much higher critical current density than the sample Kusevic et al. used [18] are available which also helps decrease the resistivity further. The resistivity of the Bi-2223 tape coil is estimated to be about 10^{-10}–$10^{-9}\,\Omega\,\mathrm{m}$.

2.3. Quality factor

Quality factor is a very important parameter to estimate the resistive loss of the RF coil and other losses. It is defined as the resonant frequency times the stored field energy divided by the power loss per circle of RF, as shown in Eq. (5) [19]:

$$Q = \omega \frac{\text{stored energy}}{P}. \tag{5}$$

The total losses of an HTS tape coil are quite different from those of an HTS film coil and a normal metal coil. The losses of a film coil include the intrinsic conductive loss in the superconductor itself, and the extrinsic losses from radiation and dielectric substrate. The losses of an HTS tape coil result from not only the intrinsic conductive loss of the tape, but also the conductive loss of the contact metal pads, loss of the capacitor soldered and the radiation loss. The final quality factor Q_0 can be expressed by the quality factors determined by different loss sources of HTS material (Q_H) radiation (Q_r), contact pad (Q_p) and capacitor (Q_c), as shown in Eq. (6):

$$\frac{1}{Q_0} = \frac{1}{Q_H} + \frac{1}{Q_r} + \frac{1}{Q_p} + \frac{1}{Q_c}. \tag{6}$$

In the interesting frequency of MRI, the radiation loss is usually neglected. As discussed above, superconductor loss may be one order lower than the copper loss in liquid nitrogen, so the contribution of Q_H to the total loss can also be neglected. Consequently, the major factors to affect Q_0 come from Q_p and Q_c. Then Eq. (6) can be converted to Eq. (7):

$$\frac{1}{Q_0} \approx \frac{1}{Q_p} + \frac{1}{Q_c}. \tag{7}$$

Compared with HTS thin films, there are lumped capacitors in the HTS tape coils, different from the pure distributed parameter structure of HTS films. Therefore, even though the RF specific capacitors with high Q_c are used, the loss caused by the capacitors is much higher than the dielectric loss from the substrates of films, specially for the cases at frequency higher than 100 MHz. Referring to the data from specifications of ATC 100B series RF Capacitors [20], Q_c of the capacitor higher than 51 pF will be less than 1000 at 150 MHz. Therefore the total quality factor Q_0 of the tape

coil will not exceed 1000 at this frequency. The loss from contact pads or solder joints should be another factor to decrease Q_0 of the tape coil, which has been discussed in Ref. [9]. So accounting for these two factors, Q_0 of a tape coil will not be more than one order higher than a copper coil in liquid nitrogen at high frequency. With respect to the low frequency tape coil, Grasso et al. [8] found that Q_0 could be even higher than that of a planar YBCO thick film [4]. However, the maximum Q_0 value only appeared during the specific sheath etching step and the process was difficult to control, so it would not be very meaningful in practice for general HTS tape coils.

When used for imaging, another parameter of the coil should be considered is the loaded quality factor Q_l, which reflects the coupling of the coil to the sample being imaged. In contrast to Q_0, which is also called unloaded quality factor Q_{ul}, Q_l is also determined by the inductive loss from the sample besides those sources mentioned above. Q_l and Q_0 often used to calculate the sample resistance (R_s) by Eq. (8):

$$R_s = \frac{1}{\omega C}\left(\frac{1}{Q_l} - \frac{1}{Q_0}\right), \tag{8}$$

where ω is the angular frequency and C is the capacitance used in the coil.

3. Experiments and results

A 5-in. tape RF receiving coil for 0.21 T low field MRI has been demonstrated and a 3-fold SNR improvement has been obtained over the room temperature copper coil by Cheng et al. [10]. However, SNR improvement with HTS tape coils applied to high field may have more significance because high field MRI has become the mainstream. A HTS tape surface coil was demonstrated for the first time for phantom imaging at 1.5 T, the most widely used high field clinical MRI system presently.

A 50 mm diameter Bi-2223 surface coil was fabricated with the Bi-2223 tape provided by Trithor Company, Germany, whose critical current density J_{c0} is 70 A/mm^2. When the tape is bended to 50 mm in diameter, J_{c0} will not decrease by over 5%. The fabrication of the Bi-2223 tape surface coil is just like the fabrication of normal surface coil, and has been described in Refs. [8,10]. Two copper coils with the same size resonated at the same frequency were fabricated for comparison. ATC 100B series high Q RF capacitors were used in both HTS tape coil and copper coils.

Accounting for the safety issue, phantom imaging was carried out instead of in vivo imaging. A cylindrical phantom with diameter of 10cm and height of 7 cm was used to simulate human muscles, whose dielectric constant and conductivity at 100 MHz are 70.5 and 0.68 S/m respectively, quite similar with the corresponding values of 72 and 0.85 S/m of human muscles [21].

Before the imaging experiment, Qs of the coils were measured by mutual coupling method with an HP 8753C network analyzer [9]. The results of the measurement were listed in Table 1. Note that Qs of the coils had to be measured out of the magnet because any electric devices were not allowed to operate in the scanner room. Accounting for the reason, the HTS tape coil resistance should be a little higher than the measured value in Table 1.

The setup of the imaging experiment is illustrated in Fig. 2. The MR scanner type is GE Signa LX 1.5 T. A custom designed glass vacuum vessel was used as cryostat. The vessel has thin vacuum gap of 5 mm, which helps to increase the filling factor, and meanwhile provides good heat insulation performance to keep liquid nitrogen for 1 h. The coils were used as transmit/receive mode at liquid nitrogen temperature (77 K). Matching was implemented by mutual coupling method with a pick up coil wrapping around the vacuum vessel. A GE spin-echo sequence with TR = 120 ms, TE = 3.4 ms, and NEX = 1 was used for all the imaging

Table 1
Resonant frequency, Q and resistance for HTS and two copper coils CC: cool copper, Cu: copper, ul: unloaded, l: loaded, R_s, sample resistance, R_c: coil resistance

	f_{ul} (MHz)	Q_{ul}	f_l (MHz)	Q_l	R_c (Ω)	R_s (Ω)
HTS	63.846	1284	63.872	418	0.031	0.065
CC	63.842	452	64.877	270	0.098	0.066
Cu	63.839	337	63.882	225	0.132	0.066

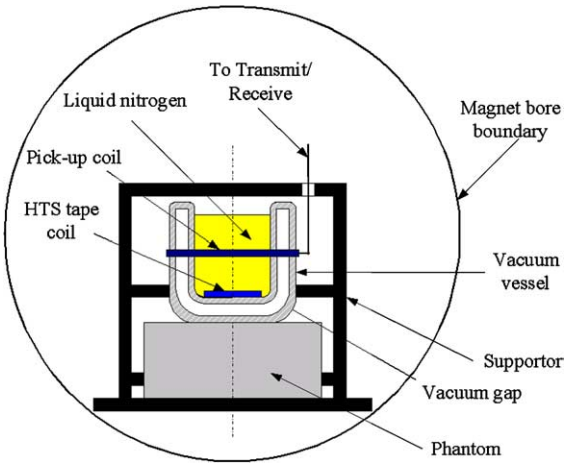

Fig. 2. Experiment setup for phantom imaging at 1.5 T.

experiments. Different power settings were determined for coils by stepping through a range of transmit attenuation values in the prescans. The optimum transmitted power was set with both HTS coil and copper coils in order to maximize the signal amplitude. The FOV, the slice thickness and acquisition matrix size were 15 cm × 15 cm, 5 mm and 256 × 256 respectively. The coronal phantom images obtained with these coils were taken from the plane about 1.4 cm depth away from the coils and were shown in Fig. 3.

The intensities of the images in Fig. 3 mapped by SNR were analyzed. The noise region was selected as the whole background in the images. The signal region was selected as the circular region just covering the phantom. Signal intensity along the horizontal axis extracted from images of the phantom with these three coils were plotted and shown in Fig. 4. The results showed that the image with the HTS tape coil obtained an average SNR improvement of 1.11-fold over the image with the cool copper coil at 77 K, and 1.36-fold over the image with the copper coil at room temperature.

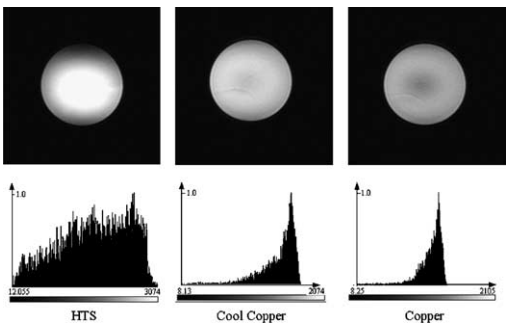

Fig. 3. Coronal phantom images and intensity histogram comparison by GE spin-echo sequence, TR = 120 ms, TE = 3.4 ms, NEX = 1. Field of view, the slice thickness and acquisition matrix size were 15 cm × 15 cm, 5 mm and 256 × 256. In the histograms, the x-axis denotes intensity and y-axis denotes normalized pixel number.

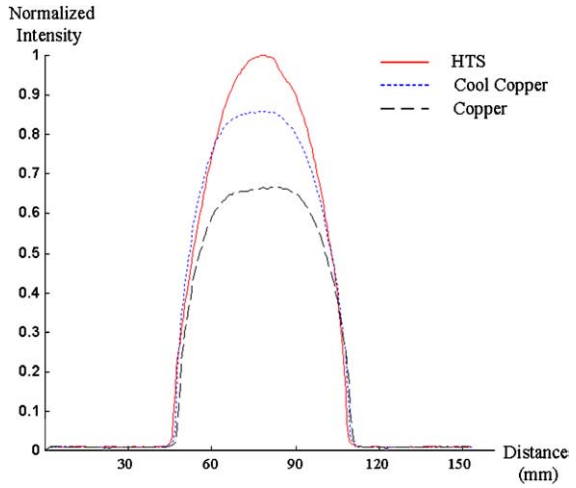

Fig. 4. Plots of intensities along the horizontal axis extracted from phantom images, in which the red, blue, black curves denote the HTS, cool copper and copper coil at room temperature, respectively.

4. Discussion

In contrast to the three times SNR improvement demonstrated with the 5-in. tape coil for 0.21 T [10], the 1.36-fold SNR improvement with the 2-in. tape coil for 1.5 T seems not so significant. The result is quite reasonable because it is considered that the sample resistance increases with the square of resonant frequency [22] while the coil resistance is proportional to resonant frequency [23]. However, both the SNR improvement at 0.21 T and the SNR improvement at 1.5 T in this experiment are higher than the prediction according to the scaling law given by Darrasse and Gine-

fri [23]. The reason relies in the model they used is based on the semi-infinite conductive sample. In practice, the SNR performances should be much dependent on the sample sizes, sample electric parameters and their coupling to the coils. Therefore the SNR improvements by HTS coils might be underestimated.

Comparing the histograms of the phantom images with three coils shown in Fig. 3, the histogram of HTS tape coil showed much wider distribution than the other two. It indicated that the sensitivity of the tape coil is much more imhomogeneous. The major reason may be a small fraction of the HTS filaments were broken during bending and etching, which caused inhomogeneous current distribution in the tape cross section. Another reason for it might be that the flip-angle adjustment during the manual scan caused small slice-profile distortion.

Another issue of non-linear power transmission with thin film coils [24] would not be encountered with respect to the HTS tape coil. Although the critical current density of HTS thin films is higher than that of tapes, the thickness of a thin film is often in nanometer magnitude, much smaller than the London penetration depth in micron magnitude. Therefore, the critical current density can actually be exceeded during pulse sequence excitation. However, the present HTS tapes provide high enough critical current density and much larger transmission cross section than thin films. Even the degradation of critical current density, J_c, of HTS tape in the high field is taken into account, its J_c is still higher than $2\,A/mm^2$ of copper. Therefore, when applied to RF excitation as transmit coil, J_c of HTS tape will seldom saturated.

To avoid non-linear transmission behavior, thin film coils are often used as receive-only mode. However, another issue of decoupling the thin film coil with the transmitter has to be addressed. Due to the intrinsic distributed structure of HTS films, decoupling circuit is difficult to be applied, which can also introduce extra losses and hence decrease SNR improvement. Meanwhile, it was reported that more noises were introduced in receive-only mode than in transmit-receive mode due to the addition of transmit volume coil [2].

Anisotropic characteristics of the type II HTS materials in the magnetic field really restricts the applications of both HTS films and tapes. In order to preserving high quality factor performance of HTS coils, correct orientation of the HTS grain with respect to the field is very important. There is still no solution to address it perfectly. For HTS tapes, the anisotropy in the magnetic field can be alleviated by decreasing the operating temperature [25] or by a novel HTS filaments arrangement of horizontal and vertical stacks [26].

So far, almost all of the HTS coil demonstrations in MRI are like once-done experiments and cannot be run routinely by inexperienced physicians. To ensure reproducible operation without complex handling constraints, HTS RF systems are highly expected to provide convenient and safe packaging of coils, friendly usage and low cost feature. At short term, it means both of HTS tape coils and thin film coils for MRI are still far from commercialization and only restricted in academic research applications.

5. Conclusion

HTS tapes used as RF coils for MRI are attractive due to their much lower cost and relatively easier operation than HTS thin films. A 50mm surface coil for 1.5 T, the most widely used clinical high field MRI, was built and applied to phantom imaging for the first time. It demonstrated a 1.11-fold SNR improvement over a cool cooper coil at 77 K and a 1.36-fold SNR improvement over a copper coil at room temperature respectively. Based on the theoretical analysis and experiment results, it is predicted that HTS tape coils would show merits on SNR performance from 0.2 T with coil size of 5-in. up to about 1.5 T with coil size smaller than 2-in. Many technical issues of HTS tape coils still need to be solved before large-scale applications for routine clinical scans.

Acknowledgments

The authors thank Thrithor Company, Germany for Bi-2223 tape sample and Dr. Xiaoyuan

Feng for the experiment in HuaShan Hospital, Shanghai, China. This project is supported by Hong Kong RGC Earmarked Research Grant HKU 7045/01E.

References

[1] R.D. Black, T.A. Early, P.B. Roemer, O.M. Mueller, A. Mogro-Campero, L.G. Turner, G.A. Johnson, Science 259 (1993) 793.
[2] J.R. Miller, S.E. Hurlston, Q.Y. Ma, W.F. Dean, D.J. Kountz, J.R. MacFall, L.W. Hedlund, G.A. Johnson, Magn. Reson. Med. 41 (1999) 72.
[3] J. Wosik, K. Nesteruk, L.M. Xie, M. Strikovski, F. Wang, J.H. Miller, J.M. Bilgen, P.A. Narayana, Physica C 341–348 (2000) 2561.
[4] S.J. Penn, N.McN. Alford, D. Bracanovic, A.A. Esmail, V. Scott, T.W. Button, IEEE Trans. Appl. Supercond. 9 (1999) 3070.
[5] J.G. van Heteren, T.W. James, L.C. Bourne, Magn. Reson. Med. 32 (1994) 396.
[6] S.E. Hurlston, W.W. Brey, S.A. Suddarth, G.A. Johnson, Magn. Reson. Med. 41 (1999) 1032.
[7] A.S. Hall, N.McN. Alford, T.W. Button, D.J. Gilderdale, K.A. Gehring, I.R. Young, Magn. Reson. Med. 20 (1991) 340.
[8] G. Grasso, A. Malagoli, N. Scati, P. Guasconi, S. Roncallo, A.S. Siri, Supercond. Sci. Technol. 13 (2000) L15.
[9] J. Yuan, G.X. Shen, Supercond. Sci. Technol. 17 (2004) 333.
[10] M.C. Cheng, K.H. Lee, K.C. Chan, K.K. Wong, E.S. Yang, ISMRM (2003) 2359.
[11] C.J. Gorter, H.B.G. Casimir, Physica 1 (1934) 306.
[12] H. Hubner, A.A. Valenzuela, Appl. Phys. Lett. 64 (1994) 3491.
[13] N.McN. Alford, T.W. Button, M.J. Adams, S. Hedges, B. Nicholson, W.A. Phillips, Nature 349 (1991) 680.
[14] M. Ciszek, S.P. Ashworth, M.P. James, B.A. Glowacki, A.M. Campbell, R. Garre, S. Conti, Supercond. Sci. Technol. 9 (1996) 379.
[15] S.K. Yip, J. Sauls, Phys. Rev. Lett. 69 (1992) 2264.
[16] A. Maeda, Y. Iino, T. Hanaguri, N. Motohira, K. Kishio, T. Fukase, Phys. Rev. Lett. 74 (1995) 1202.
[17] S. Sridhar, J.E. Mercerau, Phys. Rev. B 34 (1986) 203.
[18] I. Kusevic, E. Babic, J.R. Cooper, W.G. Wang, H.K. Liu, S.X. Dou, FIZIKA A 8 (1999) 319.
[19] R. Ludwig, P. Bretchko, RF Circuit Design: Theory and Application, Prentice-Hall, Englewood Cliffs, NJ, 2000, p. 205.
[20] Available from: <http://www.atceramics.com/pdf/100b.pdf>.
[21] G. Hartsgrove, A. Klaszewski, A. Surowiec, Bioelectromagnetics 8 (1987) 29.
[22] B.H. Suits, A.N. Garroway, J.B. Miller, J. Magn. Reson. 135 (1998) 373.
[23] L. Darrasse, J.C. Ginefri, Biochimie 85 (2003) 915.
[24] R.D. Black, T.A. Early, G.A. Johnson, J. Magn. Reson. A 113 (1995) 74.
[25] T. Kaneko, T. Hikata, M. Ueyama, A. Mikumo, N. Ayai, S. Kobayashi, N. Saga, K. Hayashi, K. Ohmatsu, K. Sato, IEEE Trans. Appl. Supercond. 9 (1999) 2465.
[26] G. Grasso, R. Flukiger, Supercond. Sci. Technol. 10 (1997) 223.